3D MHD core collapse simulations: recent insights from the Basel group

Simon Scheidegger

MICRA 2009, Copenhagen, Denmark

24/08/09

UNI BASEL

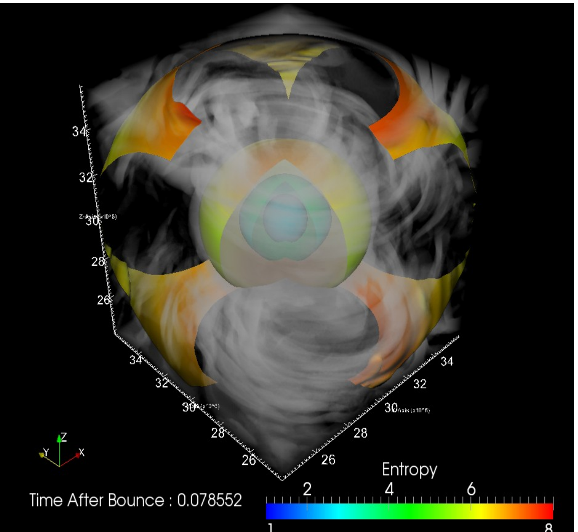

Collaborators:

T. Fischer

R. Käppeli

A. Perego

S. C. Whitehouse

Supervisor: M. Liebendörfer

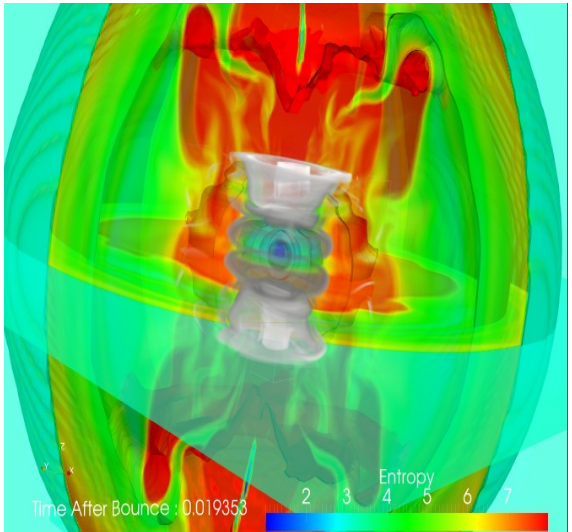

"It is (nearly) impossible to find features of the input physics in a gravitational wave signal of core collapse Supernovae

...that can be unambiguously be attributed to a specific model."

"Post bounce neutrino physics essential for quantitative prediction of GW."

Outline

-Summary of group activity

-3D MHD code with simplifications

-Recent simulation results
with respect to Gravitational waves
(Scheidegger et al. 2009, in prep.)

Ongoing efforts in 3D

T. Fischer: Quark EoS, QCD phase transition
(in collaboration with J. Schaffner-Bielich's group/Heidelberg → see I. Sagert's talk)

R. Käppeli: MHD code developement, MHD JETS
(Käppeli et al. 2009, in prep)

A. Perego: μ/τ -neutrino cooling (→see Albino's talk)

S. Scheidegger: Gravitational waves/Gravity
(Scheidegger et al. 2009, in prep)

S.C. Whitehouse:
M. Liebendörfer:
Neutrino physics
IDSA developement/implementation

(Liebendörfer et al. 2009, Whitehouse et al. 2009, in prep)

3D MHD code with simplifications

3D Hydrodynamics
Plasma physics

Parallel 3D ideal MHD code (Pen et al (2003), Liebendörfer et al. (2006), Käppeli et al. (2009), in prep)

Weak interactions
Neutrino transport

Parametrised & Deleptonisation scheme
(Liebendörfer et al. (2005), Liebendörfer et al. (2009), Whitehouse et al. (2009), in prep.)

Figure: Electron fraction profiles during core collapse in spherical symmetric reference models.

→Resulting GW quantitative for times t<5ms postbounce.

Y_e as a function of density. Y_e only weak funct. of time.
Changes in $Y_e(\rho)$ only due to e^--capture →Possible to deduce corresponding changes in entropy and calculate ν-stress from emitted neutrinos.

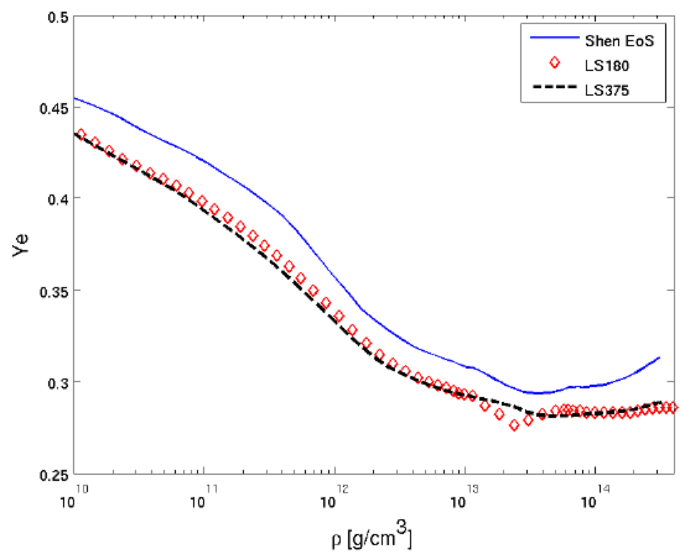

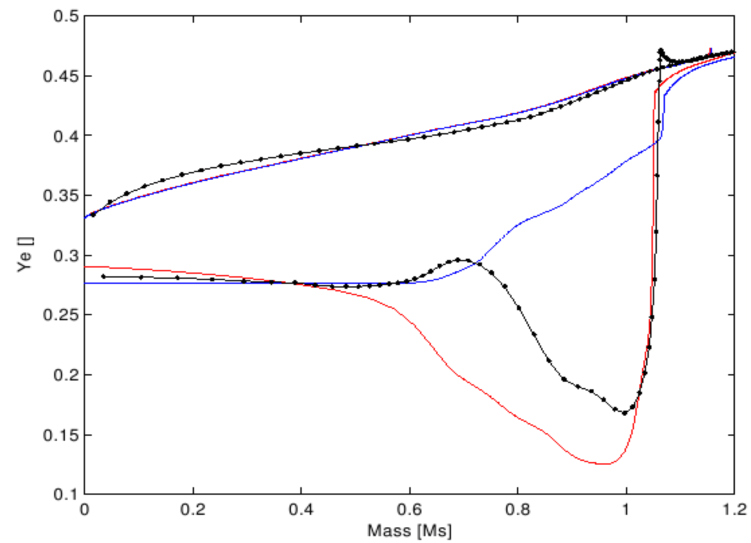

Figure: Comparison of the Ye profiles of an almost non-rotating 3D hydro models (blue lines) and a leakage model (red lines) with the spherically symmetric model based on general relativistic three-flavour Boltzmann neutrino transport at 5ms before and after bounce.

→Resulting GW quantitative for times t > 5ms postbounce.

Nuclear physics: EoS
(Lattimer & Swesty (1991), Shen et al. (1998))

General relativity: Spherical effective GR potential
(Marek et al. (2006))

Progenitor: $15 M_\odot$ (Woosley & Weaver (1995), 1D)

Simulation parameters

(25 models,with /without post bounce vs)

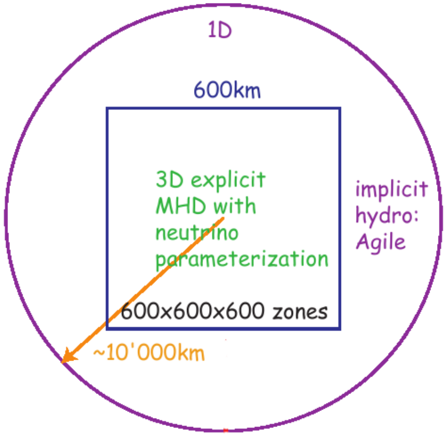

Figure: Computational domain

Figure: Cray XT-5 at CSCS

-Central cube embedded in larger spherically symmetric computational domain, treated by a 1D hydrodynamics code (Liebendörfer et al (2002))

-Variations in EoS:
LS (K=180, 220, 375 MeV), Shen EoS

-Shellular differential rotation set up:
quadratic cut off at A=500km

$$\Omega(r) = \Omega_{i,c} \cdot \frac{A^2}{A^2 + r^2}$$

-Initial magnetic fields assumed according to Heger et al. (2005),
but also “numerical” experiments.

-All simulations were carried out at **Swiss Supercomputing Centre CSCS**

-240'000 CPUh/month

What can we learn from SNe GWs?

Core collapse SN observables

-Electromagnetic radiation (Optical, X-rays, nuclear decays,...)
-Pulsar kicks
-Neutrinos
-Gravitational waves

Electromagnetic radiation:

Can probe e.g. energy, chemical composition, progenitor mass
→Not able to constrain details of the operating explosion mechanism.

Gravitational waves could probe:

- high density regime of electromagnetically hidden regions.
- Explosion mechanism itself. (Different mechanisms have different GW signatures, Ott (2009))
- Impose constraints on nonaxisymmetric SN dynamics in post bounce phase.
  (Convection/rot. Instabilities/anisotropic ν-emission,...)
- Nuclear physics (Compressibility of matter/EoS) ?

-Ultimate goal: Robust wave forms for burst data analysis

Gravitational waves wrapper

We do not assume any symmetry.
Linearized Einstein equations: GW field h_{ij}^{TT} can be resolved into two orthogonal polarisations with amplitudes A+, Ax:

$$h_{ij}^{TT}(\mathbf{X},t) = \frac{1}{R}(A_+ e_+ + A_\times e_\times).$$

$$\begin{aligned} e_+ &= e_\theta \otimes e_\theta - e_\phi \otimes e_\phi \\ e_\times &= e_\theta \otimes e_\phi + e_\phi \otimes e_\theta . \end{aligned}$$

R: distance to source; unit polarisation tensors in spherical coordinates.

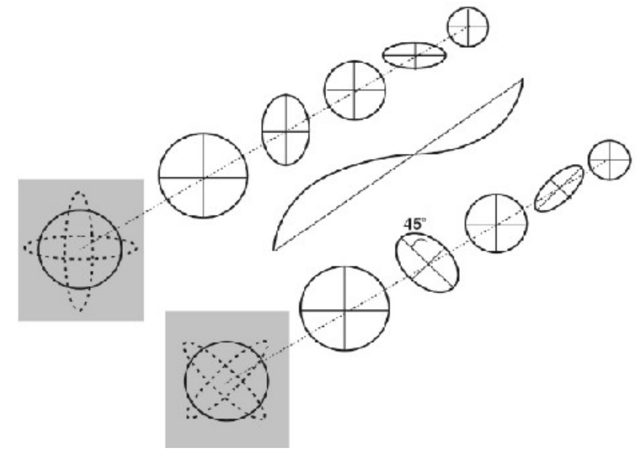

Figure: Effect of the two polarisations (+,x) on a ring of particles. The pol. act similarly, but differ by 45°

A+, Ax in first order given by linear combinations of 2nd time derivative of transverse traceless mass quadrupole tensor (Misner et al. (1973) ("Large-distance, slow-motion approximaton"))

$$\begin{aligned} A_+ &= \ddot{t}_{\theta\theta} - \ddot{t}_{\phi\phi} \\ A_\times &= 2\ddot{t}_{\theta\phi} . \end{aligned}$$

$$t_{ij}^{TT} = \frac{G}{c^4}\int dV \rho \left(x_i x_j - \frac{1}{3}\delta_{ij} r^2 \right)$$

Consider two particles on the x-axis, separated by a coordinate distance Lc

$$\begin{aligned} L &= \int_0^{L_c} dx \sqrt{g_{xx}} = \int_0^{L_c} dx \sqrt{1 + h_{xx}^{\mathrm{TT}}(t, z=0)} \\ &\simeq \int_0^{L_c} dx \left[1 + \frac{1}{2} h_{xx}^{\mathrm{TT}}(t,z=0) \right] = L_c \left[1 + \frac{1}{2} h_{xx}^{\mathrm{TT}}(t,z=0) \right] \end{aligned}$$

Fractional change in proper separation between the two particles is:

$$\frac{\Delta L}{L_c} \simeq \frac{1}{2} h_{xx}^{TT}$$ ~O(10^{-21}-10^{-22})

Figure: LIGO, Livingston. Michelson Interferometer
Other detectors: VIRGO, GEO600,TAMA300,AIGO,..

GWs from convection

(e.g. Müller & Janka (1997), Müller et al. (2004), Ott et al. (2008), Scheidegger et al. (2008), Marek et al. (2008), Ott (2009),...)

-Stellar evolution models: progenitors rotate rather slow at onset of collapse (Heger et al. (2005)).

-Non- or slowly rotating progenitors undergo quasi-spherically symmetric collapse.

-Only Hydrodynamical instabilities can cause deviations from spherical symmetry and therefore trigger GW.

-Convectively unstable regions in PNS. (Schwarzschild-Ledoux)

$$\left(\frac{\partial\rho}{\partial Y_e}\right)_{P,s}\left(\frac{\partial Y_e}{\partial r}\right)+\left(\frac{\partial\rho}{\partial s}\right)_{Y_e,s}\left(\frac{\partial s}{\partial r}\right)>0$$

-Prompt convection: As shock passes trough outer core material, it leaves behind a negative entropy gradient. Additionally, after neutrino burst, a negative lepton gradient arises in the outer part of the PNS. (e.g. Müller & Janka (1997), Dessart et al. (2006), Ott al. (2008))

-LS vs. SHEN EoS: Differences in GW signature! (but below current detector threshold!)

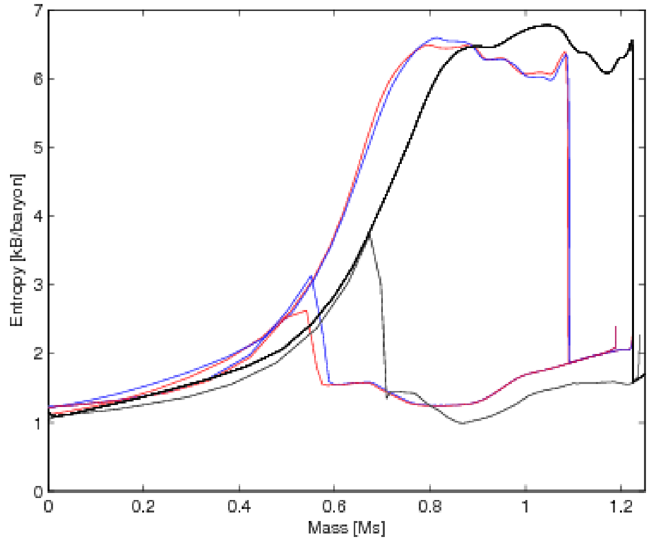

Figure: Spherically averaged radial entropy profiles from nonrotating models s15R0E1CA (red), s15R0E3CA (blue) at 0/6ms postbounce, s15R0STCA (black) at 0 and 9ms pb.

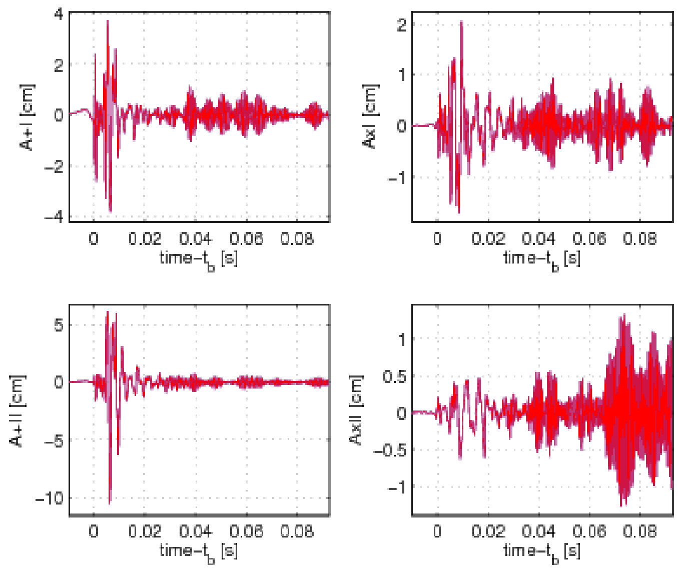

Figure: GW amplitudes of leakage model s15RE1CA$_L$.

Movie: Rotational core collapse

Movie:

Animation by J. Biddiscombe, CSCS

Initial conditions:

- $\Omega_{i,central}$=2π [rad/sec]
- β_{init}=0.26%
- β_b = 5.2%
- EoS: LS(K=180)

GW from rotational core bounce

(e.g. Müller et al. (1982),...,Kotake et al (2006),Dimmelmeier et al. (2007), Ott et al. (2007), Dimmelmeier et al (2008),...)

-Only so-called type I signal in rot. core collapse.

-GW burst signal at bounce depends primarly on precollapse central angular velocity and on the progenitor mass.
(Dimmelmeier et al. (2008), 140 2D GR models. We find similar behaviour in our smaller data-sample)

-Purely axisymmetric GW Signal.

-EoS: minor differences, hardly visible in the GW signal.

-Waveform can constrain rotation rate via combined measurement of peak amplitude and f_{Char}.

-Could verify outcome of Dimmelmeier et al. (2008) in 3D.

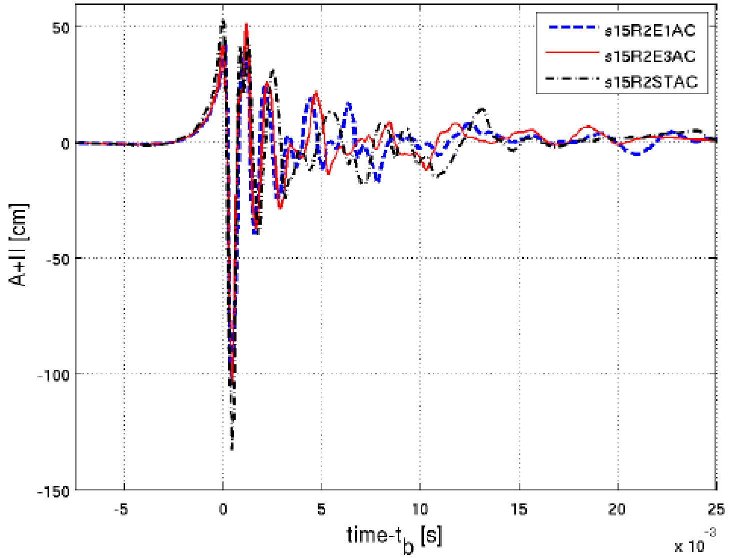

Figure: Models that differ only in the input EoS (LS180, LS375, SHEN)

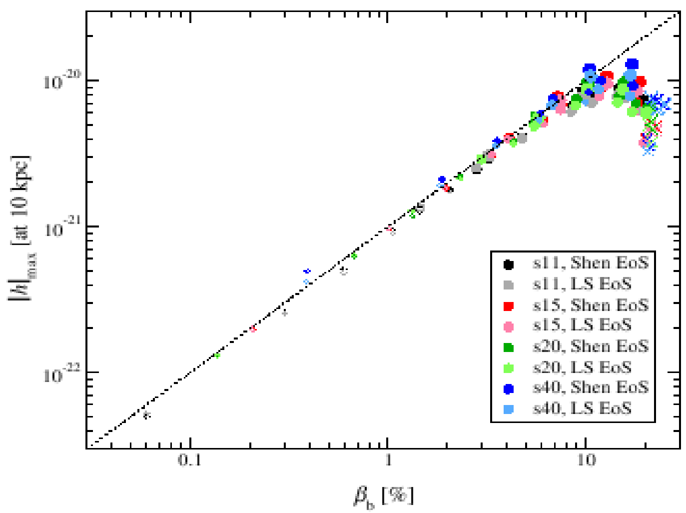

Figure: From Dimmelmeier et al.(2008)

GW from low T/|W|-instability (3D-effect)

(See e.g. Watts et al. (2005), Ou & Toholine (2006), Ott et al. (2007), Cerda-Duran et al. (2007), Scheidegger et al. (2008))

-Triggered in differentially rotating systems such as PNS.

-GW emission frequency corresponds to the eigenfrequency of the m=2 mode (2x)

-Pattern speed $\sigma_p = \sigma/m$ of unstable mode matches the local angular velocity (corotation point).

-Modes assumed to behave as: $\exp[-i(\sigma t - m\phi)]$

-GW polarisations (+,x) are phase-shifted by π/2, as one would expect of a rotating bar.

-Dominant m= 1,2 modes; scales with N cycles as $h_{\rm eff} \propto h\sqrt{N}$

-All our models with β_b > 5% become unstable.

- large degeneracy space!
- leakage models: 5-10x larger amplitudes (PNS more compact!)

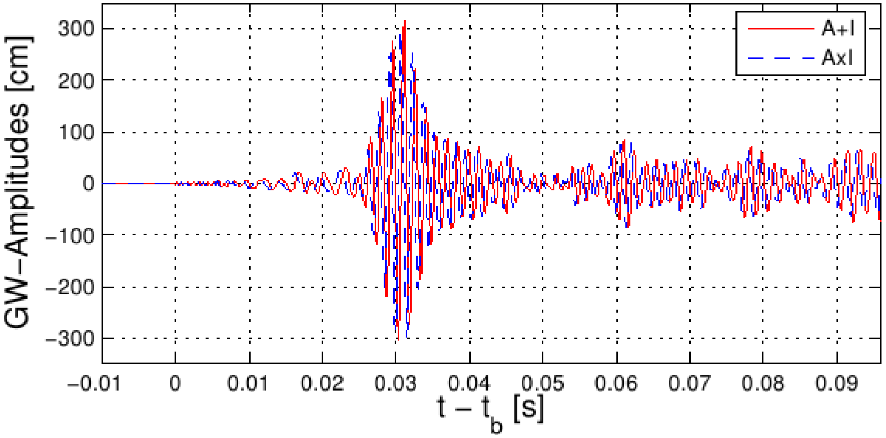

Figure: GW from low T/łWł instability, polarisations +,x in polar direction.

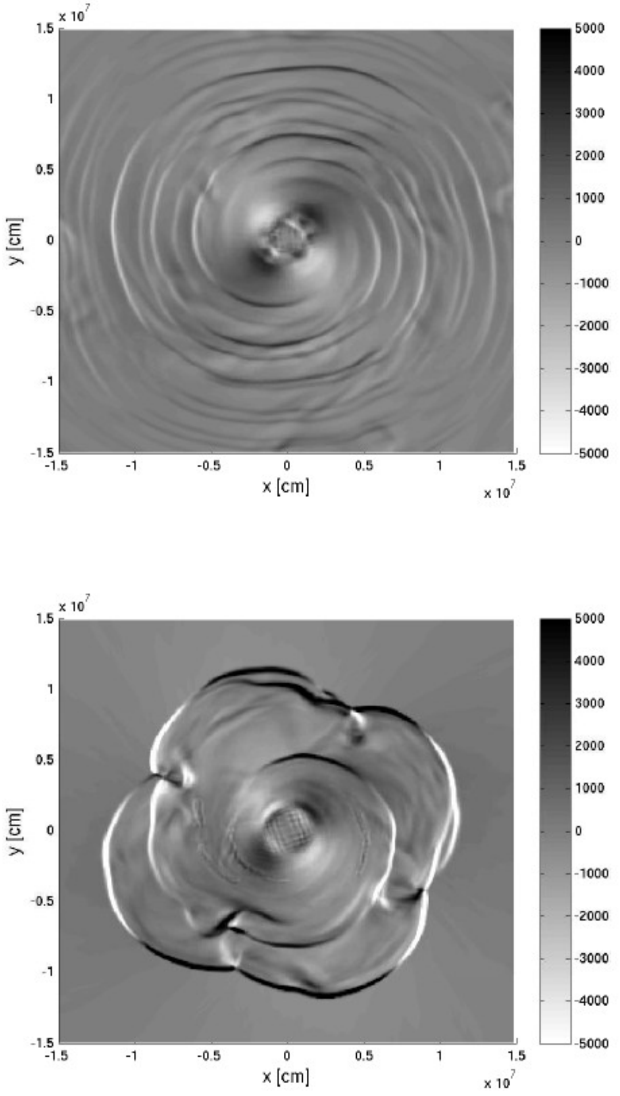

Figure: Snapshots of vorticity z-component 29ms postbounce. Note the m= 1, resp. 2 spiral arms.

Strong poloidal magnetic fields I

(e.g. Kotake et al. (2004), Obergaulinger et al. (2006), Burrows et al. 2007,Takiwaki et al. 2009, ...)

MHD Jet mechanism:

-Rapid and differential rotation

-B-field amplification: flux compression, winding of poloidal into toroidal B-field,...

-$P_{mat} \sim P_{B\text{-Field}}$

-Simulations usually start with strongly (unphysically) magnetised cores. (10^{12} G), can't resolve MRI.

-Magnetic stresses can assist or even drive matter outflow along rotational axis (JET). JET powered by the rotational energy transferred to the jet by magnetic stresses.

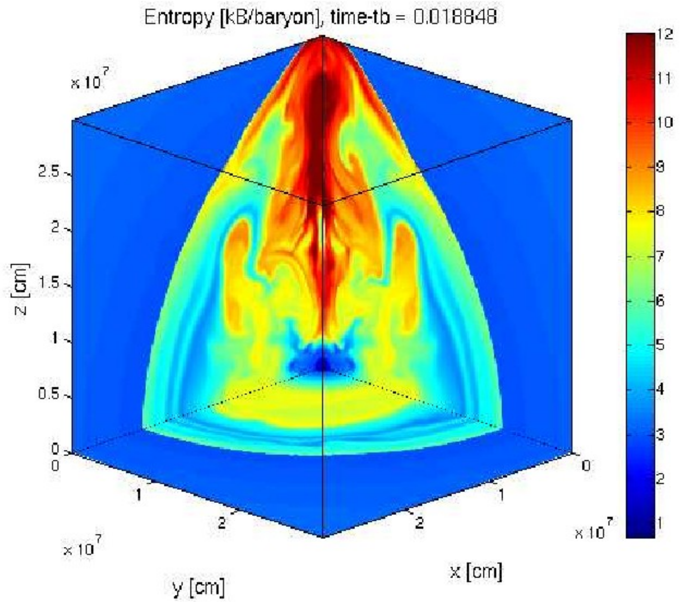

Figure: Model with strong initial poloidal B-field, 1000 x B toroidal.

Gravitational waves:

-matter outflow along z-axis causes 'memory' effect $A+II \sim 2mv_z^2$ (m grows over time)

-slowly time-varying signal (outside of LIGO window)

-Contribution of magn. energy density to GW signal

$$\eta_{mag} = \frac{\frac{B^2}{8\pi c^2}}{\rho_c} \sim 10\% \left(\frac{B_c}{\text{several} \times 10^{17}\text{G}}\right)^2 \left(\frac{\rho_c}{10^{13}\text{g/cm}^3}\right)^{-1}$$

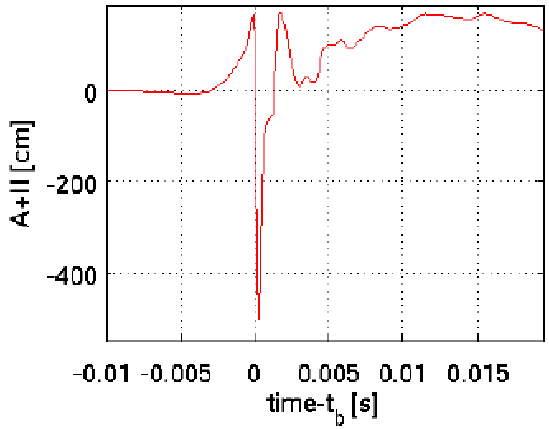

Figure: GW amplitude A+II of a Model with strong initial poloidal B-field 1000 x B toroidal.

Movie: strong toroidal magnetic field

Movie:

Initial conditions:

- $\Omega_{i,central}$=3π [rad/sec]
- β_{init}=0.26%
- β_b = 5.2%
- EoS: LS(K=180)

-$B_{pol,init}$ = 5e9 [G]

-$B_{tor,init}$ =1e12 [G]

-pb neutrino cooling

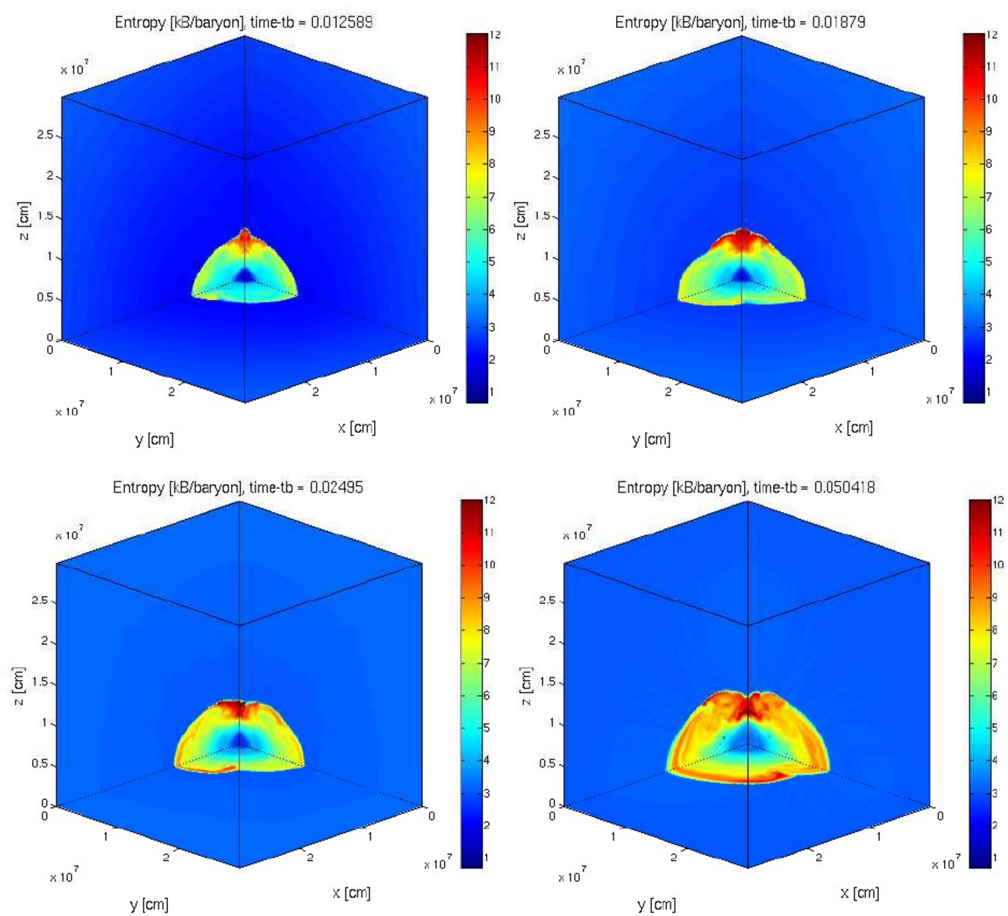

Figure: Snapshots at representative instants.

Strong toroidal magnetic fields II

-Stellar evolution calculations: (Heger et al. 2005)

Btor ~1000 x Bpol

-In 2D: configuration leads to jet (Kotake et al. 2006).

-3D: more degrees of freedom!

-Field winding not effective/fast enough.

-Non-axisymmetric Hydrodynamical instabilities

develop and redistribute hot matter.

-No Jet explosion within the

duration of our simulation.

-Subject under investigation! (Käppeli et al. 201X).

-effects of B-field on GW entirely masked.

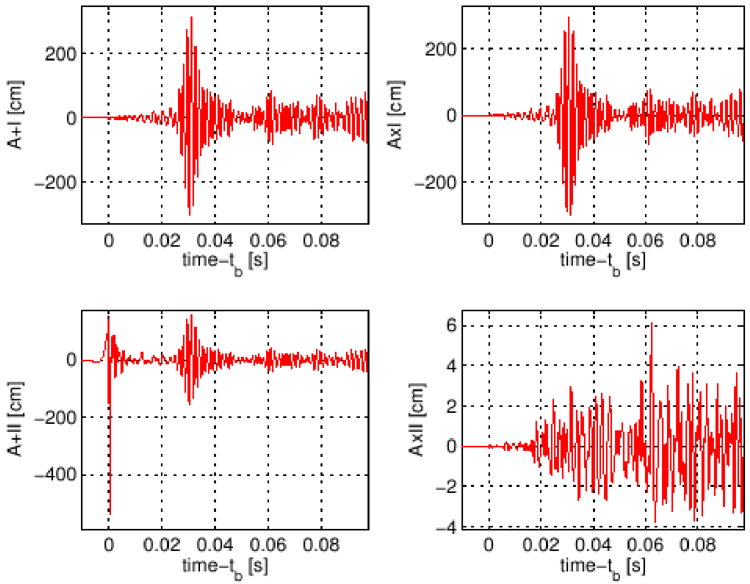

Figure: GW signature from a model with strong initial Btor.

Summary

-Covered large parameter space in 3D with respect to GW.

-First 3D MHD simulations with postbounce deleptonisation.

-Neutrino inclusion crucial for postbounce GW signal!

-SN dynamics has multiple degeneracies, reflected in GWs.

-MHD Jet mechanism needs detailed 3D investigations!

What are the initial magnetic field configurations? (from stellar evolution calculations).